

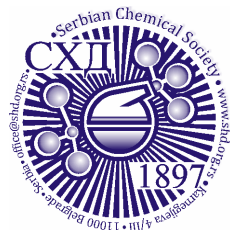


ACCEPTED MANUSCRIPT

This is an early electronic version of an as-received manuscript that has been accepted for publication in the Journal of the Serbian Chemical Society but has not yet been subjected to the editing process and publishing procedure applied by the JSCS Editorial Office.

Please cite this article as W. López-Orozco, L. H. Mendoza-Huizar, G. A. Álvarez-Romero and J. J. M. Torres-Valencia, *J. Serb. Chem. Soc.* (2024) <https://doi.org/10.2298/JSC240428074L>

This “raw” version of the manuscript is being provided to the authors and readers for their technical service. It must be stressed that the manuscript still has to be subjected to copyediting, typesetting, English grammar and syntax corrections, professional editing and authors’ review of the galley proof before it is published in its final form. Please note that during these publishing processes, many errors may emerge which could affect the final content of the manuscript and all legal disclaimers applied according to the policies of the Journal.



J. Serb. Chem. Soc. **00(0)** 1-13 (2024)
JSCS-12906

A computational study of the potential bioactivity of hibiscus and garcinia acids against SARS-CoV-2

WENDOLYNE LÓPEZ-OROZCO, LUIS HUMBERTO MENDOZA-HUIZAR*, GIAAN ARTURO ÁLVAREZ-ROMERO AND J. DE JESÚS MARTÍN TORRES-VALENCIA

Área Académica de Química, Universidad Autónoma del Estado de Hidalgo, carretera Pachuca-Tulancingo, 42184, Mineral de la Reforma, Hidalgo. México.

(Received 28 April; revised 5 June; accepted 21 August 2024)

Abstract: A computational chemical study was conducted on the diastereoisomers of hibiscus acid (HA) and garcinia acid (GA), investigating their docking capabilities with the main protease (6LU7) of SARS-CoV-2. Electrostatic potential mappings unveiled negative charges associated with the carboxyl and hydroxyl groups positioned at C-2 and C-3 for both hibiscus and garcinia acids. However, the presence of more negative potentials around C-2 and C-3 of hibiscus acid, compared to garcinia acid, suggests that substituents in the (2*S*,3*R*) configuration possess a stronger electron-attracting capacity than those in the (2*S*,3*S*) configuration. Molecular docking studies indicated that both hibiscus acid and garcinia acid bind to the main protease through the catalytic pocket. Nonetheless, molecular dynamics simulations revealed that only HA remained bound to the active site for 100 ns with an RMSD of less than 1 Å, whereas GA dissociated from the complex within the initial 16 ns. These findings illuminate the differential binding behaviors of the two compounds, with implications for potential therapeutic interventions against SARS-CoV-2. These findings shed light on the differential binding behaviors of the two compounds, holding implications for potential therapeutic interventions against SARS-CoV-2.

Keywords: 6LU7; hibiscus; molecular docking; molecular dynamics.

INTRODUCTION

The rapid spread of the COVID-19 pandemic over the past three years has highlighted the urgent need for developing effective treatments for this and other diseases. This is possible, if effective and specific drugs are available against specific viruses or bacteria. Nevertheless, it is well known that the design and synthesis of specific drugs may take several decades. Different strategies have been employed in the discovery of antiviral drugs against COVID-19.¹ These

* Corresponding author. E-mail: hhuizar@uaeh.edu.mx
<https://doi.org/10.2298/JSC240428074L>

strategies encompass drug repurposing, where approved or investigational drugs are utilized beyond their original indications, alongside high-throughput screening, computer-assisted virtual screening, and structure-based drug discovery among others.¹⁻³ In this regard, natural sources like plants and fruits may contain bioactive compounds that have antiviral, antibiotic, or antiinflammatory properties useful against different diseases.^{4,5} It could lead to the development of alternative treatments, which may become more accessible and affordable in a shorter time. Thus, research on medicinal compounds of natural origin may lead to the discovery of substances with antiviral or immunomodulatory properties, which could be crucial for the development of effective treatments against SARS-CoV-2 and its variants.⁵⁻¹²

Phytochemicals derived from *Hibiscus sabdariffa*¹³⁻²² and compounds extracted from *Garcinia* species,^{23,24,33,25-32} have been analyzed employing experimental and computational approaches because have shown therapeutic potential against SARS-CoV2.⁵⁻¹² In this sense, it has been reported that the *Garcinia Kola*, *Garcinia cambogia*, *Garcinia mangostana*, and *Hibiscus Sabdariffa* extracts are able to reduce cytokine storms during the late phase of SARS-CoV-2 infections by decreasing S1-glycoprotein secretion.^{16,23} In addition, the therapeutic use of *Hibiscus Sabdariffa* in controlling the inflammatory response against COVID-19 by blocking the ACE-2 receptor has been proposed because it contains a number of compounds structurally similar to hydroxychloroquine and mannose,^{15,16,34} that could act as agonists for ACE2 and MLB receptors.¹⁵ Also, *in silico* studies have allowed for the analysis of the interactions of bioactive compounds like manggiferin present in *Garcinia mangostana* with the receptors spike RDM, helicase, 3CLpro, and RdRp of SARS-CoV-2,^{24,28,35-37} and the biomolecules present in *Hibiscus Sabdariffa* with 3CLpro and PLppo,^{13,16-18,20,22}. In summary, the results indicate that various molecules from *Hibiscus sabdariffa* and *Garcinia* species exhibit strong binding affinity to the main proteases of SARS-CoV-2, suggesting their potential therapeutic use against SARS-CoV-2 infection.

Specifically, hibiscus acid (HA) ((2*S*,3*R*)-3-hydroxy-5-oxooxolane-2,3-dicarboxylic acid), see Figure 1a, which is found in *Hibiscus sabdariffa*,³⁸ and *Hibiscus schizopetalus*,³⁹ and garcinia acid (GA) ((2*S*,3*S*)-3-hydroxy-5-oxooxolane-2,3-dicarboxylic acid)), see Figure 1b (present in *Garcinia cambogia*),^{38,40} have been shown to have a vasorelaxant effect in addition to inhibiting the neuraminidase of influenza.^{41,42} Also, it has recently been reported that their anti-inflammatory and antioxidant properties are able to treat the symptoms of COVID-19.^{16,20,22} Additionally, isolated HA has proven to be neither clastogenic nor cytotoxic,³⁸ whereas *Garcinia kola* extract has shown antigenotoxic activity and the ability to repair damage caused by mutagenic agents.²³ Thus, in this study, we analyze the binding of HA and GA to the

Mprotease of SARS-CoV-2 through molecular docking to identify whether HA and GA are suitable candidates for acting as antiviral medicines against SARS-CoV-2. Additionally, we conduct dynamic molecular (MD) studies. We believe that this research may prove valuable in understanding the role of HA and GA in inhibiting the ACE2 receptor for SARS-CoV-2.

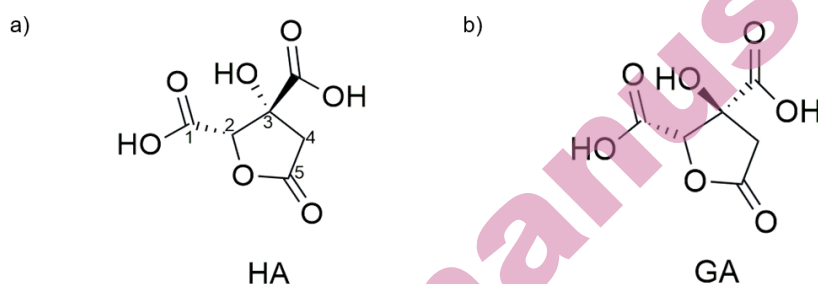


Fig. 1 Chemical structure of hibiscus acid ((2S,3R)-3-hydroxy-5-oxooxolane-2,3-dicarboxylic acid) and garcinia acid ((2S,3S)-3-hydroxy-5-oxooxolane-2,3-dicarboxylic acid).

EXPERIMENTAL

The HA and GA structures were subjected to full geometrical optimization employing the B3LYP/6-311G (d,p) level of theory.⁴³ Vibrational frequencies were calculated to ensure that the stationary points corresponded to a minimum on the potential energy surface. Protein-ligand docking studies of the HA and GA ligands with the 3CL-M^{pro} enzyme of SARS-CoV-2 (PDB ID: 6LU7) were performed via the web server SwissDock.⁴⁴ Visualizations of the protein-ligand complex were performed through the programs Chimera,⁴⁵ and Discovery Studio Visualizer 2019,⁴⁶ while molecular dynamics calculation and visualization were performed using the programs GROMACS,⁴⁷ and VMD,⁴⁸ respectively. The OPLS/AA force field was employed in all of the MD simulations.⁴⁹ To perform the MD study, a simulation box was generated, and the complex protein-ligand was placed in the center of the box. At least 1.0 nm from the rim of the protein ligand to the boundary of the cubic box was kept and it was filled with water molecules modelled using the TIP₃P equation.⁵⁰ Also, 4 Na⁺ ions for both molecules were added to the simulation box to equilibrate the charges in the system. The integration of the motion equations was performed at a time step of 2 fs with fully periodic boundary conditions (PBC). Prior to the MD simulation, an energy minimization process was performed to ensure a reasonable starting structure in terms of geometry and solvent orientation. Then equilibration was conducted in two stages. The first one was conducted under an NVT ensemble until the temperature of the system reached a plateau at the desired value. In the second one, the equilibrium of pressure was conducted under an NPT ensemble for 1 ns. Then a MD for 100 ns was conducted to analyze the stability of the protein-ligand complex.

RESULTS AND DISCUSSION

Lipinski's rule of five and ADMET prediction

By predicting the physicochemical and pharmacological properties of compounds, it is possible to evaluate the ability of molecules as potential drugs using parameters related to their oral bioavailability and their administration in the

body. Lipinsky's rule of five and the ADMET parameters of HA and GA were evaluated using ADMETlab 2.0,⁵¹ see Table 1. HA and GA obey Lipinsky's rule of five, which includes the following properties (optimal values in parentheses),⁵²: logP de -0.40 y -0.33 (<5), number of AHB hydrogen bond acceptors of 7 (<10), number of DHB hydrogen bond donors equal to 3 and 3 (<5), number of rotational bonds equal to 2 (<10), and molecular weight of 190 g / mol (<500). On the other hand, the two acids showed Caco-2 permeability and total clearance values lower than the limit. However, they do not show hepatotoxicity, mutagenicity, oral toxicity in rats, or carcinogenicity. Also, they have a good half-life. Finally, for their metabolism, it was predicted that the acids would act as substrates for the cytochrome P450 C9 subtype.

Table 1. *In silico* study of the ADMET properties of hibiscus acid and garcinia acid.

Property	Model name	Optimum value	Hibiscus acid	Garcinia acid
Absorption	Caco-2 permeability	>-5.15 (log Papp en10 ⁻⁶ cm/s)	-6.105	-6.139
	Intestinal absorption (human)	% Absorbed	0.176	0.029
Distribution	Plasma protein binding	<90 %	13.24	15.37
	Volume distribution	0.04-20 L / Kg	0.218	0.281
Metabolism	CYP2A2 Inhibitor	Categorical (Yes/No)	No	No
	CYP2A2 Substrate	Categorical (Yes/No)	No	No
	CYP2C19 Inhibitor	Categorical (Yes/No)	No	No
	CYP2C19 Substrate	Categorical (Yes/No)	No	No
	CYP2C9 Inhibitor	Categorical (Yes/No)	No	No
	CYP2C9 Substrate	Categorical (Yes/No)	Yes	Yes
	CYP2CD6 Inhibitor	Categorical (Yes/No)	No	No
	CYP2CD6 Substrate	Categorical (Yes/No)	No	No
	CYP3A4 Inhibitor	Categorical (Yes/No)	No	No
	CYP3A4 Substrate	Categorical (Yes/No)	No	No
Excretion	Clearance	High >15	1.894	2.176
		Moderate 5-15		
		Low <5 (log ml/min/kg)		
T _{1/2}		Long half-life > 3h	0.825	0.727
		Short half-life < 3h		
Toxicity	Human hepatotoxicity	Category: positive, negative	Negative	Negative
	AMES toxicity	Category: positive, negative	Negative	Negative
	Rat oral acute toxicity	Low 0	0.01	0.011
		High 1 (log mg/kg_bw/day)		
Carcinogenicity	Probability	0.009	0.014	

Analysis of interfering compounds

Molecules that contain substructures with a high potential to interfere with biological assays are known as Pan-assay interference compounds (PAINS).⁵³ Although this is not valid in all cases, care should be taken if an active compound

contains some substructures.⁵³ In this sense, there are databases that allow the comparison of compounds with known PAIN molecules. In the present work, the structures of hibiscus acid and garcinia acid were analyzed using the ZINC database,⁵⁴ and no interfering structures or substructures were identified in either case.

Mapping of the electrostatic potentials

Understanding the electrostatic potential of molecules is crucial for elucidating their interaction mechanisms, especially in the context of ligand-protein binding. Electrostatic interactions play a significant role in molecular recognition and binding processes. Figure 2 shows the MEP of the molecules hibiscus acid and garcinia acid evaluated at the B3LYP/6-311G (d,p) level of theory. In this figure, the negative potential areas (red color) represent electron-abundant zones, while the positive potential areas (blue color) show a relative lack of electrons. Note the presence of negative potential areas, particularly around the carboxyl and hydroxyl groups, which suggests regions of high electron density that could participate in interactions with positively charged residues on the protein surface. From figure 2, the carboxyl and hydroxyl groups at C-2 and C-3 of HA exhibit more negative potential values than those of GA, indicating that the substituents in the (2*S*,3*R*) conformation are more electrophilic compared to those in the (2*S*,3*S*) conformation.

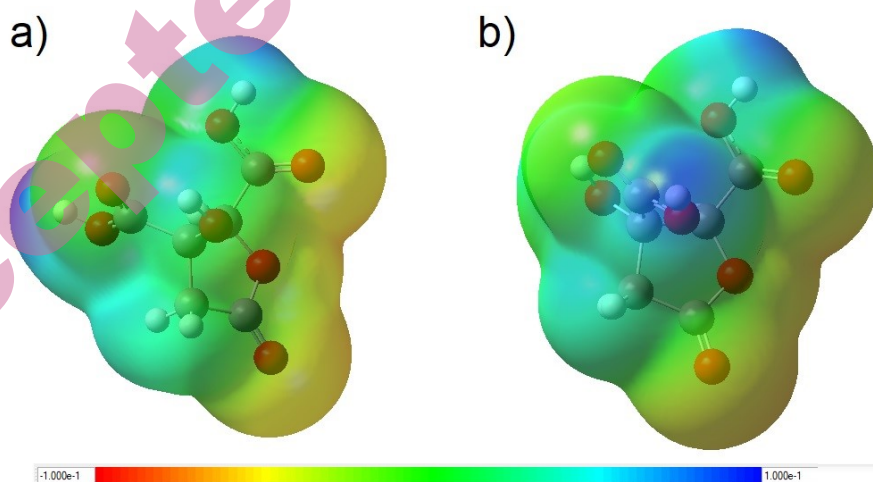


Fig. 2 Mapping of the electrostatic potentials evaluated at the B3LYP/6-311G (d,p) level of

theory on a density isosurface (valor = 0.002 e/a.u.³) for a) HA and b) GA

Docking study

In order to analyze the ability of HA and GA to inhibit the replication of SARS-CoV-2, A molecular docking study was performed to study the binding of HA and GA to the main protease (6LU7) of this virus, see Figures 3 and 4. Since 6LU7 has been identified as a target for inhibition of viral replication, Fig. 3a shows the HA-6LU7 configuration, where the binding energy was $-6.76 \text{ kcal mol}^{-1}$ and Fig. 4a shows the GA-6LU7 configuration. Garcinia acid interacts with 6LU7 with a binding energy of $-6.93 \text{ kcal mol}^{-1}$. These binding energy values compare favorably with those found for caffeoylshikimic acid, chlorogenic acid, cianidanol, and kaempferol when they are docked with strong affinity to the 3CLpro main protease of SARS-CoV-2.¹³ Also, the delta energy binding may be associated with the formation of different numbers of hydrogen bonds and interactions between ligand and receptor, caused by the change in the orientation of the carbonyl substituent in HA and GA diastereoisomers. Similar behavior has been observed in the case of diastereomers of nelfnavir, which are identified as potent inhibitors of dimeric SARS-CoV-2 Mpro,⁵⁵ hydrazones trans-E and cis-E when docked into the binding pocket of 7BQY protease,⁵⁶ and redemsivir diastereoisomeric derivatives.⁵⁷ In this sense, the Gibbs energy of binding between an antigen and its receptor is of great relevance for the interaction and entry of a virus into its host on the cell surface.⁵⁸⁻⁶² Due to infecting a host cell, the virus must have an antigen with a negative Gibbs energy of binding to the host cell receptor, e.g., the glycoprotein in the receptor for SARS-CoV-2.⁶³ According to biothermodynamics, the Gibbs free energy of binding involved in virus-host interactions at the membrane level can help to better understand these interactions.⁵⁸ Thus, a higher Gibbs free energy of binding results in a faster binding rate, more rapid entry of viruses into host cells, and therefore increased infectivity.⁶² Based on the above and the fact that HA and GA show negative Gibbs binding energy with 6LU7, it is possible to suggest that these diastereoisomers can bind to 6LU7 to inhibit the SARS-COV-2 virus. In addition, the interactions around 3 Å were identified, and a 2D plot was performed as shown in Fig. 3b and 4b. It is observed that hibiscus acid and garcinia acid have van der Waals interactions with residues of the catalytic site of 6LU7 reported,⁶⁴ ASN142, HSD163, MET165, and GLU166. Interestingly, the (2S,3S) conformation of garcinia acid improves the complex interactions and favors hydrogen bond stabilization with PHE140[O-H...N], and the catalytic dyad residue CYS145[O...N] with a distance of 4.74 and 4.13 Å.

Molecular dynamics simulation study

To analyze whether the HA-6LU7 and GA-6LU7 complexes derived from the docking study are stable, we performed a molecular dynamics study at 100 ns. Figure 5 depicts the docked structures at 0 and 100 ns,

respectively, for the docking of garcinia acid at the 6LU7 site. It is clear that GA is not stable at the initial pocket site (see Figures 5a-b), because GA docked at the original site (Fig 5a), and at the end of 100 ns, it docked at a new site (see Figure 5b). This can also be seen in the RMSD plot (Fig 5c), where at approximately 16 ns the RMSD increases significantly, greater than 3 Å, suggesting the mobilization of garcinia acid away from another active site, which has not been identified with the associated site in 6LU7 to prevent SARS-COV-2 virus replication.

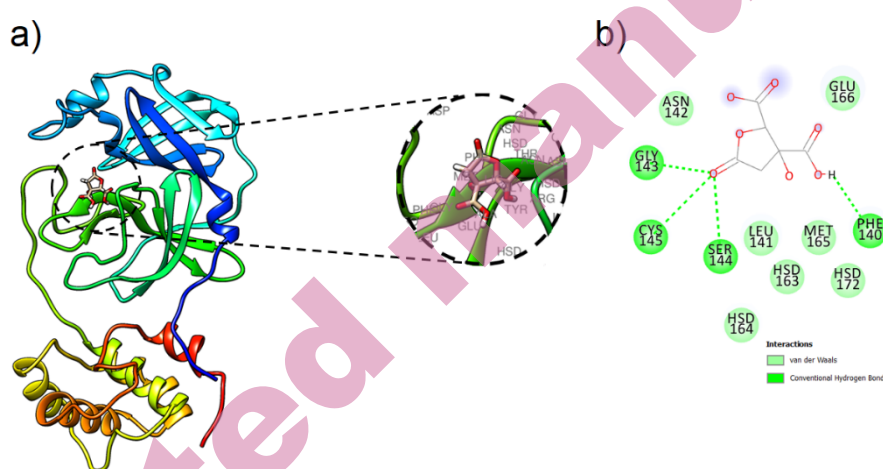


Fig. 3 a) HA binding site in the 6LU7 of SARS-CoV-2, b) 2D mapping of ligand/6LU7 configuration interactions for HA

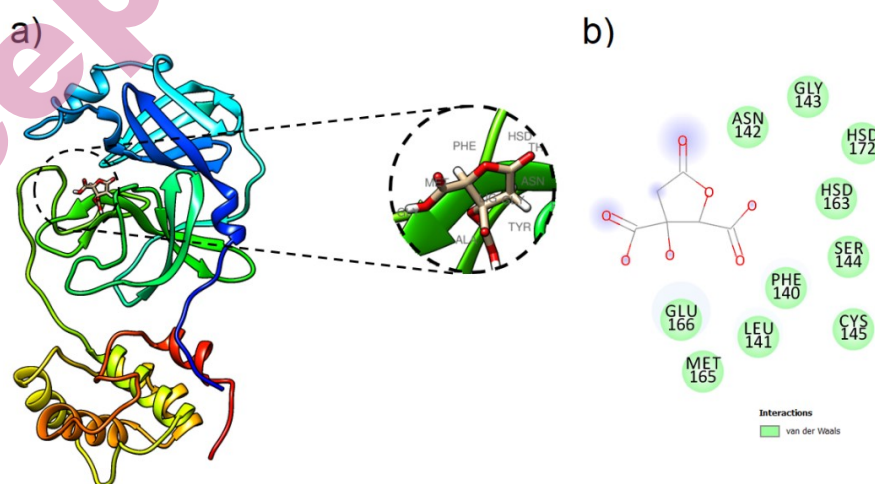


Fig. 4 a) GA binding site in the 6LU7 of SARS-CoV-2, b) 2D mapping of ligand/6LU7 configuration interactions for GA.

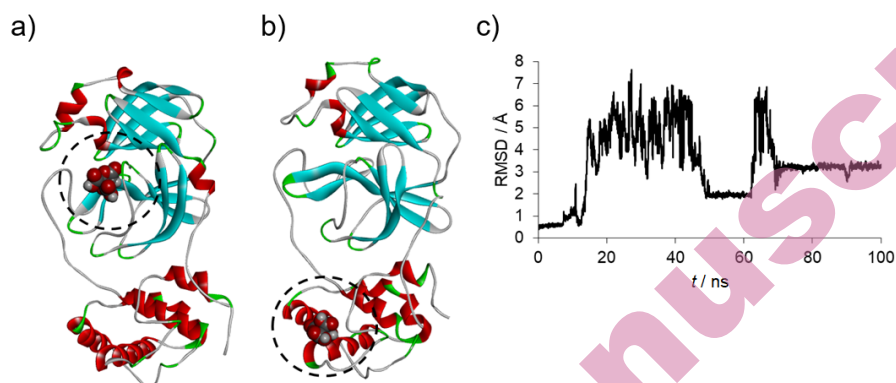


Fig. 5 Molecular dynamics simulation results for GA, a) initial docking configuration, b) docking configuration at 100 ns, and c) The RMSD profile depicts the equilibrium trajectory of the GA-6LU7 complex through 100 ns.

In the case of the HA-6LU7 complex, in Figure 6, the structures HA docked at 6LU7 are shown at 0 and 100 ns, respectively. It is clear that HA remains in the pocket site during the 100 ns, suggesting that the complex formed is stable (see Figures 6a-b). The last one is corroborated by the RMSD graph (Fig. 6c), which shows that the RMSD is less than 1 Å. The last results suggest the formation of the HA-6LU7 complex is stable.

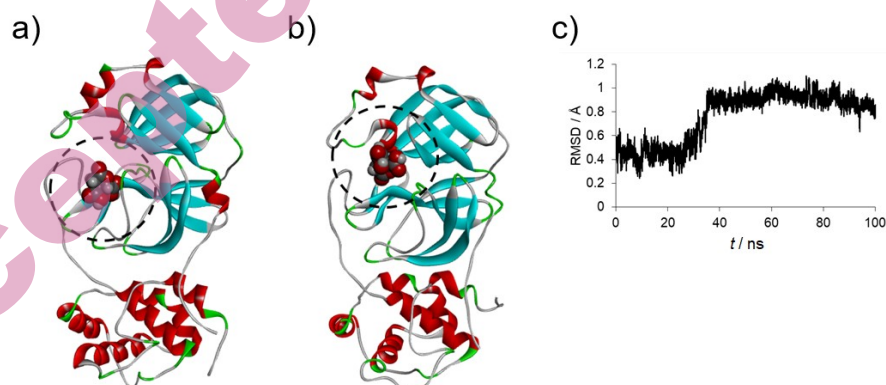


Fig. 6 Molecular dynamics simulation results for HA, a) initial docking configuration, b) docking configuration at 100 ns, and c) The RMSD profile depicts the equilibrium trajectory of the HA-6LU7 complex through 100 ns.

In addition, Figure 7 shows the behavior of the potential energy of the complexes during the MD simulation. It can be seen that the potential energies of the GA-6LU7 and HA-6LU7 complexes are in the range of -9.49×10^5 to -9.43×10^5 kJ mol⁻¹ and reach a constant level from the beginning of the simulation. The latter

illustrates the energetically stable nature of the GA-6LU7 and HA-6LU7 complexes.

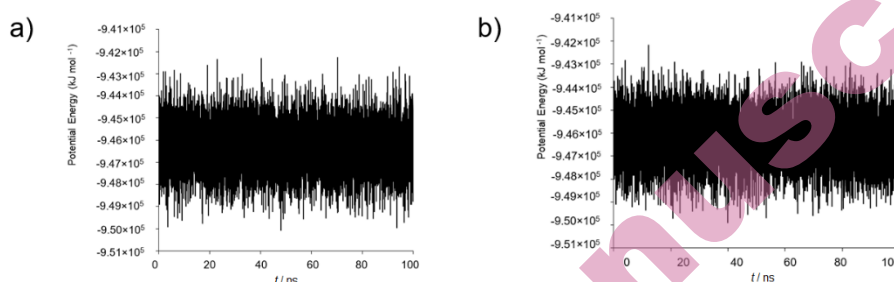


Fig 7 Potential energy graph illustrates the energetically stability of a) GA and b) HA

CONCLUSION

Binding pose and binding energy were also analyzed for the HA-6LU7 and GA-6LU7 configurations, where the formation of the complex at the active site position was confirmed, with binding energies equal to $-6.76 \text{ kcal mol}^{-1}$ and $-6.93 \text{ kcal mol}^{-1}$, respectively. Analysis of the interactions between HA and GA with 6LU7 revealed that HA shows Van der Waals-type interactions with ASN142, HSD163, MET165, and GLU166, and in the case of garcinia acid, the interactions were with residues PHE140 [O-H.N] and CYS145 [O-H.N.]. Finally, by molecular dynamics simulation, it was possible to verify the permanence of hibiscus acid in the active site of 6LU7, whereas garcinia acid did not remain in the protease active site.

Acknowledgements: WLO acknowledges CONACYT for the scholarship granted for Doctoral studies. L. H. M. H. thankfully acknowledges the computer resources, technical expertise and support provided by the Laboratorio Nacional de Supercomputo del Sureste de México, CONACYT member of the network of National laboratories through the project No. 202203072N. The authors thank to the Universidad Autónoma del Estado de Hidalgo for the funding granted for this work through Project PAO-2022-1389 UAEH. LHMH, GAAR and JJMTV acknowledge to the SNI for the distinction of his membership and the stipend received.

ИЗВОД

РАЧУНАРСКА СТУДИЈА ПОТЕНЦИЈАЛНЕ БИОАКТИВНОСТИ ХИБИСКУСНЕ И ГАРСИНИЈСКЕ КИСЕЛИНЕ ПРОТИВ SARS-COV-2

WENDOLYNE LÓPEZ-OROZCO, LUIS HUMBERTO MENDOZA-HUIZAR, GIAAN ARTURO ÁLVAREZ-ROMERO AND J. DE JESÚS MARTIN TORRES-VALENCIA

Área Académica de Química, Universidad Autónoma del Estado de Hidalgo, carretera Pachuca-Tulancingo, 42184, Mineral de la Reforma, Hidalgo. México.

Рачунарско хемијска студија је проведена на дијастереоизомерима хибискусне (НА) и гарсинијске (ГА) киселине, истражијући њихове способности доковања са главном протеазом (6LU7) од SARS-CoV-2. Мапирања електростатских потенцијала су открила да су

негативна наелектрисања придружена карбоксилним и хидроксилним групама на положајима С-2 и С-3 и за хибискусну и за гарсинијку киселину. Међутим, присуство негативнијег потенциала око С-2 и С-3 код хибискусне киселине, у поређењу са гарсинијском киселином, сугерише да супституенти у (2S,3R) поседују јачи електрон-привлачни капацитет од оних у (2S,3S) конфигурацији. Студије молекулског докинга указују да се и хибискусна и гарсинијска киселина везују за главну протеазу путем каталитичког цепа. Ипак, симулације молекулске динамике откривају да само (НА) остаје везана за активно место током 100 ns са RMSD мањом од 1 Å, док (GA) дисосује из комплекса унутар почетних 16 ns. Ови налази расветљавају различито везивно понашање два једињења, са импликацијом потенцијалне терапијске интервенције против SARS-CoV-2. Ови налази бацају светло на различито везивно понашање два једињења, подржавајући импликације за потенцијалне терапијске интервенције против SARS-CoV-2.

(Примљено 28. априла; ревидирано 5. јуна; прихваћено 21. августа 2024.)

REFERENCES

1. T. I. Ng, I. Correia, J. Seagal, D. A. DeGoey, M. R. Schrimpf, D. J. Hardee, E. L. Noey, W. M. Kati, *Viruses* **14** (2022) 961 (<http://dx.doi.org/10.3390/V14050961>)
2. Y. L. Ng, C. K. Salim, J. J. H. Chu, *Pharmacol. Ther.* **228** (2021) 107930 (<http://dx.doi.org/10.1016/J.PHARMTHERA.2021.107930>)
3. C. L. Bellera, M. Llanos, M. E. Gantner, S. Rodriguez, L. Gavernet, M. Comini, A. Talevi, *Expert Opin. Drug Discov.* **16** (2021) 605–612 (<http://dx.doi.org/10.1080/17460441.2021.1863943>)
4. I. Aanouz, A. Belhassan, K. El-Khatibi, T. Lakhlifi, M. El-Idrissi, M. Bouachrine, *J. Biomol. Struct. Dyn.* **39** (2021) 2971–2979 (<http://dx.doi.org/10.1080/07391102.2020.1758790>)
5. S. Yagi, A. Yagi, *Curr. Tradit. Med.* **9** (2023) 39-54 (<http://dx.doi.org/10.2174/2215083809666230206114117>)
6. A. Ghosh, S. Chakraborty, S. Majumder, M. Bhattacharya, *Lett. Appl. NanoBioScience* **12** (2023) 26–32 (<http://dx.doi.org/10.33263/LIANBS124.108>)
7. M. T. Quimque, K. I. Notarte, X. A. Adviento, M. H. Cabunoc, V. N. de Leon, F. S. L. delos Reyes, E. J. Lugtu, J. A. Manzano, S. N. Monton, J. E. Muñoz, K. D. Ong, D. Y. Pilapil, V. Roque, S. M. Tan, J. A. Lim, A. P. Macabeo, *Comb. Chem. High Throughput Screen.* **26** (2021) 459–488 (<http://dx.doi.org/10.2174/1386207325666210917113207>)
8. R. B. Malabadi, K. P. Kolkar, N. T. Meti, R. K. Chalannavar, *Int. J. Innov. Sci. Res. Rev.* **3** (2021) 1507–1517. (<https://journalijisr.com/sites/default/files/issues-pdf/IJISRR-600.pdf>)
9. Y. T. M. Alharbi, W. M. Abdel-Mageed, O. A. Basudan, R. A. Mothana, M. Tabish Rehman, A. A. ElGamal, A. S. Alqahtani, O. I. Fantoukh, M. F. AlAjmi, *Saudi Pharm. J.* **32** (2024) 102023 (<http://dx.doi.org/10.1016/J.JSPS.2024.102023>)
10. M. Ariefin, R. R. Saputra, I. N. Pramesti, *AIP Conf. Proc.* **3055** (2024) 040001 (<https://doi.org/10.1063/5.0193646>)
11. S. T. Selvan, M. K. D. Jothinathan, *Cureus* **16** (2024) 1-10. (<http://dx.doi.org/10.7759/CUREUS.57151>)
12. M. A. Khanfar, M. I. Saleh, *Curr. Med. Chem.* **16**(3) (2024) e57151 (<http://dx.doi.org/10.2174/0109298673271674231109052709>)

13. E. Akbaba, D. Karatas, *J. Inst. Sci. Tech.* **13** (2023) 872–888 (<http://dx.doi.org/10.21597/jist.1187616>)
14. S. Das, S. Satapathy, D. Acharya, S. Kumar Sahu, *Res. Sq.* **2023** (2023) 1–12 (<http://dx.doi.org/10.21203/RS.3.RS-2837087/V1>)
15. C. Parga-Lozano, *Duazary* **17** (2020) 1–3 (<http://dx.doi.org/10.21676/2389783x.3597>)
16. C. H. Parga-Lozano, *Biomed. J. Sci. Tech. Res.* **35** (2021) 28000–28004 (<http://dx.doi.org/10.26717/bjstr.2021.35.005761>)
17. N. Balmeh, S. Mahmoudi, N. Mohammadi, A. Karabedianhajiabadi, *Informatics Med. Unlocked* **20** (2020) 100407 (<http://dx.doi.org/10.1016/J.IMU.2020.100407>)
18. S. Mahmoudi, N. Balmeh, N. Mohammadi, T. Sadeghian-Rizi, *Avicenna J. Med. Biotechnol.* **13** (2021) 107 (<http://dx.doi.org/10.18502/AJMB.V13I3.6370>)
19. N. Ohta, K. Inokuma, K. Miyabayashi, M. Miyake, I. Yagi, *Electrochemistry* **78** (2012) 132–135 (<http://dx.doi.org/10.5796/electrochemistry.78.132>)
20. N. F. Ramadhani, A. P. Nugraha, D. Rahmadhani, M. S. Puspitaningrum, Y. Rizqianti, V. D. Kharisma, T. N. E. B. T. A. Noor, R. D. Ridwan, D. S. Ernawati, A. P. Nugraha, *J. Pharm. Pharmacogn. Res.* **10** (2022) 418–428 (http://dx.doi.org/10.56499/jppres21.1316_10.3.418)
21. S. Guardiola, N. Mach, *Endocrinol. y Nutr.* **61** (2014) 274–295 (<http://dx.doi.org/10.1016/j.endonu.2013.10.012>)
22. E. Shawky, A. A. Nada, R. S. Ibrahim, *RSC Adv.* **10** (2020) 27961–27983 (<http://dx.doi.org/10.1039/d0ra05126h>)
23. O. A. Olajide, V. U. Iwuanyanwu, I. Lepiarz-Raba, A. A. Al-Hindawi, M. A. Aderogba, H. L. Sharp, R. J. Nash, *Phyther. Res.* **35** (2021) 6963–6973 (<http://dx.doi.org/10.1002/ptr.7315>)
24. H. Y. Aati, A. Ismail, M. E. Rateb, A. M. AboulMagd, H. M. Hassan, M. H. Hetta, *Plants* **11** (2022) 2521 (<http://dx.doi.org/10.3390/PLANTS11192521>)
25. A. J. Akindele, A. Sowemimo, F. O. Agunbiade, M. O. Sofidiya, O. Awodele, O. Ade-Ademilua, I. Orabueze, I. O. Ishola, C. I. Ayolabi, O. B. Salu, M. O. Akinleye, I. A. Oreagba, *Nat. Prod. Commun.* **17** (2022) 1–43 (<https://doi.org/10.1177/1934578X221096968>)
26. O. P. Abodunrin, O. F. Onifade, A. E. Adegboyega, *Informatics Med. Unlocked* **31** (2022) 100964 (<http://dx.doi.org/10.1016/J.IMU.2022.100964>)
27. D. Muralitharan, V. Varadharajan, B. Venkidasamy, *J. Mol. Recognit.* **36** (2023) e3055 (<http://dx.doi.org/10.1002/JMR.3055>)
28. N. S. Aini, V. D. Kharisma, M. H. Widyananda, A. A. A. Murtadlo, R. T. Probojati, D. D. R. Turista, M. B. Tamam, V. Jakhmola, E. Yuniarti, S. Al Aziz, M. R. Ghifari, M. T. Albari, R. S. Mandeli, M. A. Ghifari, D. Purnamasari, B. Oktavia, A. P. Lubis, F. Azra, F. Fitri, A. N. M. Ansori, M. Rebezov, R. Zainul, *Pharmacogn. J.* **14** (2022) 575–579 (<http://dx.doi.org/10.5530/pj.2022.14.138>)
29. A. N. M. Ansori, V. D. Kharisma, A. A. Parikesit, F. A. Dian, R. T. Probojati, M. Rebezov, P. Scherbakov, P. Burkov, G. Zhdanova, A. Mikhalev, Y. Antonius, M. R. F. Pratama, N. I. Sumantri, T. H. Sucipto, R. Zainul, *Pharmacogn. J.* **14** (2022) 85–90 (<http://dx.doi.org/10.5530/pj.2022.14.12>)
30. V. D. Kharisma, A. N. M. Ansori, Y. Antonius, I. Rosadi, A. A. A. Murtadlo, V. Jakhmola, M. Rebezov, N. Maksimiuk, E. Kolesnik, P. Burkov, M. Derkho, P. Scherbakov, M. E. Ullah, T. H. Sucipto, H. Purnobasuki, *J. Pharm. Pharmacogn. Res.* **11** (2023) 743–756 (http://dx.doi.org/10.56499/JPPRES23.1650_11.5.743)

31. O. A. Kolawole, T. G. Femi, O. E. Kolawole, O. O. Monisola, O. Temitope, A. B. Benjamin, A. S. Adewale, S. Banj, *Nat Sci* **18** (2020) 78–85 (<http://dx.doi.org/10.7537/marsnsj180920.10>)
32. A. Kalita, M. Das, B. Das, M. R. Baro, *Beni-Suef Univ. J. Basic Appl. Sci.* **11** (2022) 1–17 (<http://dx.doi.org/10.1186/S43088-022-00214-2/FIGURES/10>)
33. N. Khamthong, N. Hutadilok-Towatana, *Nat. Prod. Commun.* **12** (2017) 453–460 (<http://dx.doi.org/10.1177/1934578x1701200337>)
34. G. I. P. Pozos, M. A. Ruiz-López, J. F. Z. Nátera, C. Á. Moya, L. B. Ramírez, M. R. Silva, R. R. Macías, P. M. García-López, R. G. Cruz, E. S. Pérez, J. J. V. Radillo, *Appl. Sci.* **10** (2020) 560 (<http://dx.doi.org/10.3390/app10020560>)
35. P. M. Afladhanti, M. D. Romadhan, H. A. Hamzah, Q. Bhelqis, *Sriwij. J. Med.* **5** (2022) 31–40 (<http://dx.doi.org/10.32539/SJM.V5I1.127>)
36. A. N. M. Ansori, V. D. Kharisma, A. A. Parikesit, F. A. Dian, R. T. Probojati, M. Rebezov, P. Scherbakov, P. Burkov, G. Zhdanova, A. Mikhalev, Y. Antonius, M. R. F. Pratama, N. I. Sumantri, T. H. Sucipto, R. Zainul, *Pharmacogn. J.* **14** (2022) 85–90 (<http://dx.doi.org/10.5530/PJ.2022.14.12>)
37. D. Ganjewala, H. Bansal, R. Mittal, G. Srivastava, *Herb. Med. A Boon Heal. Hum. Life* (2022) 471–500 (<http://dx.doi.org/10.1016/B978-0-323-90572-5.00012-3>)
38. J. A. Izquierdo-Vega, D. A. Arteaga-Badillo, M. Sánchez-Gutiérrez, J. A. Morales-González, N. Vargas-Mendoza, C. A. Gómez-Aldapa, J. Castro-Rosas, L. Delgado-Olivares, E. Madrigal-Bujaidar, E. Madrigal-Santillán, *Biomedicines* **8** (2020) 100 (<http://dx.doi.org/10.3390/B10MEDICINES8050100>)
39. R. A. El-Shiekh, U. R. Abdelmohsen, H. M. Ashour, R. M. Ashour, *Antibiotics* **9** (2020) 756 (<http://dx.doi.org/10.3390/antibiotics9110756>)
40. L. O. Chuah, W. Y. Ho, B. K. Beh, S. K. Yeap, *Evidence-Based Complement. Altern. Med.* **2013** (2013) 751658 (<http://dx.doi.org/10.1155/2013/751658>)
41. S. Kim, Y. Kim, J. W. Kim, Y. Hwang, S. H. Kim, Y. H. Jang, *J. Life Sci.* **32** (2022) 375–390 (<https://doi.org/10.5352/JLS.2022.32.5.375>)
42. Y. Takeda, Y. Okuyama, H. Nakano, Y. Yaoita, K. Machida, H. Ogawa, K. Imai, *Food Environ. Virol.* **12** (2020) 9–19 (<http://dx.doi.org/10.1007/s12560-019-09408-x>)
43. R. Krishnan, J. S. Binkley, R. Seeger, J. A. Pople, *J. Chem. Phys.* **72** (1980) 650–654 (<http://dx.doi.org/10.1063/1.438955>)
44. A. Grosdidier, V. Zoete, O. Michielin, *Nucleic Acids Res.* **39** (2011) W270 (<http://dx.doi.org/10.1093/NAR/GKR366>)
45. E. F. Pettersen, T. D. Goddard, C. C. Huang, G. S. Couch, D. M. Greenblatt, E. C. Meng, T. E. Ferrin, *J. Comput. Chem.* **25** (2004) 1605–1612 (<http://dx.doi.org/10.1002/jcc.20084>)
46. Biovia Dassault Systèmes, *Discovery Studio Visualiser 2019*, Dassault Systèmes, San Diego, 2020 (<http://dx.doi.org/https://discover.3ds.com/discovery-studio-visualizer-download>)
47. C. Kutzner, S. Páll, M. Fechner, A. Esztermann, B. L. De Groot, H. Grubmüller, *J. Comput. Chem.* **36** (2015) 1990–2008 (<http://dx.doi.org/10.1002/JCC.24030>)
48. J. V. Vermaas, D. J. Hardy, J. E. Stone, E. Tajkhorshid, A. Kohlmeyer, *J. Chem. Inf. Model.* **56** (2016) 1112–1116 (<http://dx.doi.org/10.1021/acs.jcim.6b00103>)
49. W. L. Jorgensen, D. S. Maxwell, J. Tirado-Rives, *J. Am. Chem. Soc.* **118** (1996) 11225–11236 (<http://dx.doi.org/10.1021/ja9621760>)

50. W. L. Jorgensen, J. Chandrasekhar, J. D. Madura, R. W. Impey, M. L. Klein, *J. Chem. Phys.* **79** (1983) 926–935 (<http://dx.doi.org/10.1063/1.445869>)
51. G. Xiong, Z. Wu, J. Yi, L. Fu, Z. Yang, C. Hsieh, M. Yin, X. Zeng, C. Wu, A. Lu, X. Chen, T. Hou, D. Cao, *Nucleic Acids Res.* **49** (2021) W5–W14 (<http://dx.doi.org/10.1093/nar/gkab255>)
52. C. A. Lipinski, *Drug Discov. Today Technol.* **1** (2004) 337–341 (<http://dx.doi.org/10.1016/J.DDTEC.2004.11.007>)
53. J. L. Dahlin, M. A. Walters, *Assay Drug Dev. Technol.* **14** (2016) 168–174 (<http://dx.doi.org/10.1089/adt.2015.674>)
54. J. J. Irwin, K. G. Tang, J. Young, C. Dandarchuluun, B. R. Wong, M. Khurelbaatar, Y. S. Moroz, J. Mayfield, R. A. Sayle, *J. Chem. Inf. Model.* **60** (2020) 6065–6073 (<http://dx.doi.org/10.1021/ACS.JCIM.0C00675>)
55. M. Sargolzaei, *J. Mol. Graph. Model.* **103** (2021) 107803 (<http://dx.doi.org/10.1016/j.jmgm.2020.107803>)
56. M. A. Said, D. J. O. Khan, F. F. Al-Blewi, N. S. Al-Kaff, A. A. Ali, N. Rezki, M. R. Aouad, M. Hagar, *Vaccines* **9** (2021) 1012 (<https://doi.org/10.3390/vaccines9091012>)
57. A. Marques Da Fonseca, A. Luthierre, G. Cavalcante, R. Mateus, M. Carvalho, J. Falcão Do Amaral, R. P. Colares, E. S. Marinho, M. M. Neto, P. Colares, *Int. J. Res.-GRANTHAALAYAH* **8** (2020) 164–174 (<http://dx.doi.org/10.29121/GRANTHAALAYAH.V8.I11.2020.2342>)
58. P. Gale, *Microb. Risk Anal.* **21** (2022) 100198 (<http://dx.doi.org/10.1016/j.mran.2021.100198>)
59. M. Popovic, *Vaccines* **10** (2022) 2112 (<http://dx.doi.org/10.3390/vaccines10122112>)
60. M. Popovic, J. H. Martin, R. J. Head, *Heliyon* **9** (2023) e17174 (<http://dx.doi.org/10.1016/j.heliyon.2023.e17174>)
61. P. Gale, *Microb. Risk Anal.* **16** (2020) 100140 (<http://dx.doi.org/10.1016/j.mran.2020.100140>)
62. M. E. Popović, G. Šekularac, M. Popović, *Microb. Risk Anal.* **26** (2024) 100290 (<http://dx.doi.org/10.1016/J.MRAN.2024.100290>)
63. J. M. Casasnovas, T. A. Springer, *J. Biol. Chem.* **270** (1995) 13216–13224 (<http://dx.doi.org/10.1074/jbc.270.22.13216>)
64. Z. Jin, X. Du, Y. Xu, Y. Deng, M. Liu, Y. Zhao, B. Zhang, X. Li, L. Zhang, C. Peng, Y. Duan, J. Yu, L. Wang, K. Yang, F. Liu, R. Jiang, X. Yang, T. You, X. Liu, X. Yang, F. Bai, H. Liu, X. Liu, L. W. Guddat, W. Xu, G. Xiao, C. Qin, Z. Shi, H. Jiang, Z. Rao, *Nature* **582** (2020) 289–293 (<http://dx.doi.org/10.1038/S41586-020-2223-Y>).